

3. SYMMETRY ASPECTS OF PHASE TRANSITIONS, TWINNING AND DOMAIN STRUCTURES

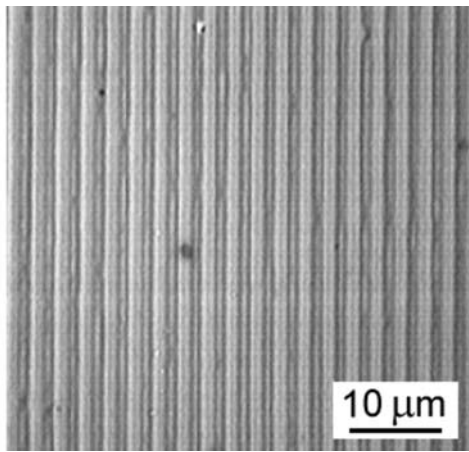


Fig. 3.4.4.3. Engineered periodic non-ferroelastic ferroelectric stripe domain structure within a lithium tantalate crystal with symmetry descent $\bar{6} \supset 3$. The domain structure is revealed by etching and observed in an optical microscope (Shur *et al.*, 2001). Courtesy of VI. Shur, Ural State University, Ekaterinburg.

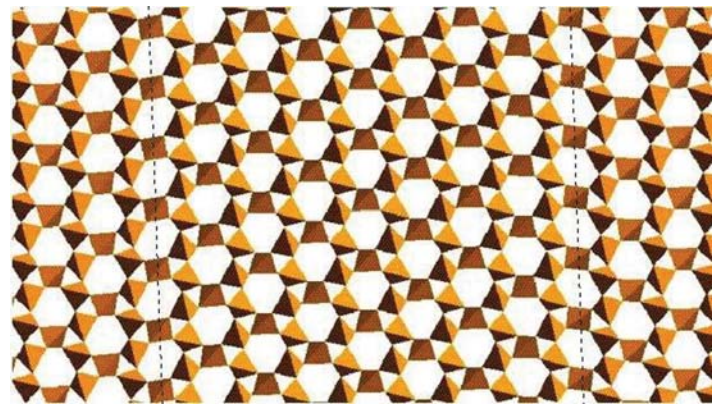


Fig. 3.4.4.4. Microscopic structure of two domain states and two parallel mutually reversed domain walls in the α phase of quartz. The left-hand vertical dotted line represents the domain wall W_{12} , the right-hand line is the reversed domain wall W_{21} . To the left of the left-hand line and to the right of the right-hand line are domains with domain state S_1 , the domain between the lines has domain state S_2 . For more details see text. Courtesy of M. Calleja, University of Cambridge.

Example 3.4.4.2. Domain walls in the α phase of quartz. Quartz (SiO_2) undergoes a structural phase transition from the parent β phase (symmetry group $6_2 2_x 2_y$) to the ferroic α phase (symmetry $3_2 2_x$). The α phase can appear in two domain states S_1 and S_2 , which have the same symmetry $F_1 = F_2 = 3_2 2_x$. The symmetry J_{12} of the unordered domain pair $\{S_1, S_2\}$ is given by $J_{12}^* = 3_2 2_x \cup 2_y^* \{3_2 2_x\} = 6^* 2_x 2_y^*$.

Table 3.4.4.5 summarizes the results of the symmetry analysis of domain walls (twins). Each row of the table contains data for one representative domain wall $W_{12}(\mathbf{n}_{12})$ from one orbit $GW_{12}(\mathbf{n}_{12})$. The first column of the table specifies the normal \mathbf{n} of the wall plane p , further columns list the layer groups \widehat{F}_{12} , T_{12} and \bar{J}_{12} that describe the symmetry properties and classification of the wall (defined in Table 3.4.4.3), and n_w is the number of symmetry-equivalent domain walls [*cf.* equation (3.4.4.21)].

The last two columns give possible components of the spontaneous polarization \mathbf{P} of the wall $W_{12}(\mathbf{n})$ and the reversed wall $W_{21}(\mathbf{n})$. Except for walls with normals $[001]$ and $[100]$, all walls are polar, *i.e.* they can be spontaneously polarized. The reversal of the polarization in reversible domain walls requires the reversal of domain states. In irreversible domain walls, the reversal of W_{12} into W_{21} is accompanied by a change of the polarization \mathbf{P} into \mathbf{P}' , which may have a different absolute value and direction different to that of \mathbf{P} .

The structure of two domain states and two mutually reversed domain walls obtained by molecular dynamics calculations are depicted in Fig. 3.4.4.4 (Calleja *et al.*, 2001). This shows a projection on the ab plane of the structure represented by SiO_4 tetrahedra, in which each tetrahedron shares four corners. The threefold symmetry axes in the centres of distorted hexagonal channels and three twofold symmetry axes (one with vertical orientation) perpendicular to the threefold axes can be easily seen. The two vertical dotted lines are the wall planes p of two mutually reversed walls $[S_1[010]S_2] = W_{12}[010]$ and $[S_2[010]S_1] =$

$W_{21}[010]$. In Table 3.4.4.5 we find that these walls have the symmetry $T_{12}[010] = T_{21}[010] = 2_x 2_y^* 2_z^*$, and in Fig. 3.4.4.4 we can verify that the operation 2_x is a ‘side-reversing’ operation $\underline{2}_{12}$ of the wall (and the whole twin as wall), operation 2_y^* is a ‘state-exchanging operation’ r_{12}^* and the operation 2_z^* is a non-trivial ‘side-and-state reversing’ operation \underline{t}_{12}^* of the wall. The walls $W_{12}[010]$ and $W_{21}[010]$ are, therefore, symmetric and reversible walls.

During a small temperature interval above the appearance of the α phase at 846 K, there exists an incommensurate phase that can be treated as a regular domain structure, consisting of triangular columnar domains with domain walls (discommensurations) of negative wall energy σ (see *e.g.* Dolino, 1985). Both theoretical considerations and electron microscopy observations (see *e.g.* Van Landuyt *et al.*, 1985) show that the wall normal has the $[uv0]$ direction. From Table 3.4.4.5 it follows that there are six equivalent walls that are symmetric but irreversible, therefore any two equivalent walls differ in orientation.

This prediction is confirmed by electron microscopy in Fig. 3.4.4.5, where black and white triangles correspond to domains with domain states S_1 and S_2 , and the transition regions between black and white areas to domain walls (discommensurations). To a domain wall of a certain orientation no reversible wall appears with the same orientation but with a reversed order of black and white. Domain walls in homogeneous triangular parts of the structure are related by 120 and 240° rotations and carry, therefore, parallel spontaneous polarizations; wall orientations in two differently oriented blocks (the middle of the right-hand part and the rest on the left-hand side) are related by 180° rotations about the axis 2_x in the plane of the photograph and are, therefore, polarized in antiparallel directions (for more details see Saint-Gregoire & Janovec, 1989; Snoeck *et al.*, 1994). After cooling down to room temperature, the wall energy becomes positive and the regular domain texture changes into a coarse domain struc-

Table 3.4.4.5. Symmetry properties of domain walls in α quartz

$$|\mathbf{P}| \neq |\mathbf{P}'|, P_i \neq -P_i, i = x, y, z.$$

\mathbf{n}	\widehat{F}_{12}	T_{12}	\bar{J}_{12}	Classification	n_w	$\mathbf{P}(W_{12})$	$\mathbf{P}(W_{21})$
$[001]$	3_z	$3_z 2_y^*$	$6^* 2_x 2_y^*$	SR	2		
$[100]$	2_x	$2_x 2_y^* 2_z^*$	$2_x 2_y^* 2_z^*$	SI	3		
$[010]$	1	2_x^*	$2_x 2_y^* 2_z^*$	SR	6	$0, 0, P_z$	$0, 0, -P_z$
$[0vw]$	1	1	2_x	AR	12	P_x, P_y, P_z	$P_x, -P_y, -P_z$
$[u0w]$	1	2_y^*	2_y^*	SI	6	$0, P_y, 0$	$0, -P_y', 0$
$[uv0]$	1	2_z^*	2_z^*	SI	6	$0, 0, P_z$	$0, 0, P_z'$
$[uvw]$	1	1	1	AI	12	P_x, P_y, P_z	P_x', P_y', P_z'